



RESEARCH ARTICLE

Inhibition of GPR120 signaling in intestine ameliorates insulin resistance and fatty liver under high-fat diet feeding

 Takuma Yasuda,¹
 Norio Harada,¹ Tomonobu Hatoko,¹ Atsuhiko Ichimura,² Eri Ikeguchi-Ogura,¹ Yuki Murata,¹ Naoki Wada,¹ Sakura Kiyobayashi,¹ Shunsuke Yamane,¹ Akira Hirasawa,³ and  Nobuya Inagaki^{1,4}

¹Department of Diabetes, Endocrinology and Nutrition, Graduate School of Medicine, Kyoto University, Kyoto, Japan; ²Department of Biological Chemistry, Graduate School of Pharmaceutical Sciences, Kyoto University, Kyoto, Japan; ³Department of Genomic Drug Discovery Science, Graduate School of Pharmaceutical Sciences, Kyoto University, Kyoto, Japan; and ⁴P.I.I.F. Tazuke-Kofukai Medical Research Institute, Kitano Hospital, Osaka, Japan

Abstract

G protein-coupled receptor (GPR) 120 is expressed in enteroendocrine cells secreting glucagon-like peptide-1 (GLP-1), glucose-dependent insulinotropic polypeptide/gastric inhibitory polypeptide (GIP), and cholecystokinin (CCK). Although GPR120 signaling in adipose tissue and macrophages has been reported to ameliorate obesity and insulin resistance in a high long-chain triglyceride (LCT) diet, intestine-specific roles of GPR120 are unclear. To clarify the metabolic effect of GPR120 in the intestine, we generated intestine-specific GPR120-knockout ($GPR120^{int-/-}$) mice. In comparison with floxed GPR120 (WT) mice, $GPR120^{int-/-}$ mice exhibited reduced GIP secretion and CCK action without change of insulin, GLP-1, or peptide YY (PYY) secretion after a single administration of LCT. Under a high-LCT diet, $GPR120^{int-/-}$ mice showed a mild reduction of body weight and substantial amelioration of insulin resistance and fatty liver. Moreover, liver and white adipose tissue (WAT) of $GPR120^{int-/-}$ mice exhibited increased Akt phosphorylation and reduced gene expression of suppressor of cytokine signaling (SOCS) 3, which inhibits insulin signaling. In addition, gene expression of inflammatory cytokines in WAT and lipogenic molecules in liver were reduced in $GPR120^{int-/-}$ mice. These findings suggest that inhibition of GPR120 signaling in intestine ameliorates insulin resistance and fatty liver under high-LCT diet feeding.

NEW & NOTEWORTHY We generated novel intestine-specific GPR120-knockout ($GPR120^{int-/-}$) mice and investigated the metabolic effect of GPR120 in the intestine. $GPR120^{int-/-}$ mice exhibited a reduction of GIP secretion and CCK action after a single administration of LCT. Under a high-LCT diet, $GPR120^{int-/-}$ mice showed mild improvement in obesity and marked amelioration of insulin resistance and hepatic steatosis. Our results indicate an important role of intestinal GPR120 on insulin resistance and hepatic steatosis.

fatty liver; GPR120; inflammatory cytokine; insulin resistance; long-chain triglycerides

INTRODUCTION

The number of obese individuals is rapidly increasing around the world (1). Obesity results from energy balance dysregulation derived partly from excessive fat intake (2). Ingestible fats consist mainly of long-chain triglycerides (LCTs); overaccumulation of LCTs leads to hepatic steatosis and insulin resistance, both of which are closely linked to cardiovascular disease, cancer, and death (3–5). To prevent the onset and exacerbation of such lifestyle-related diseases, receptors and hormones involved in digestion, absorption, and accumulation of LCTs have drawn much attention recently (6, 7).

Among the various receptors for LCTs, G protein-coupled receptor 120 (GPR120)/free fatty acid receptor (FFAR) 4 has

been increasingly studied. GPR120, a receptor for long-chain free fatty acids (LCFAs), couples mainly with Gq protein to increase intracellular Ca^{2+} levels (8, 9). GPR120 is expressed in the intestine, adipose tissue, lung, spleen, and macrophages (9, 10). Inhibition of GPR120 signaling exacerbates obesity and insulin resistance under high-LCT diet-feeding conditions (11). Studies of GPR120 agonist and global GPR120-knockout mice have shown that GPR120 signaling suppresses tumor necrosis factor (TNF)- α and lipopolysaccharide-induced inflammation in macrophages and adipose tissue and ameliorates high-LCT diet-induced obesity and insulin resistance (12–14).

In intestine, GPR120 is highly expressed in enteroendocrine cells including L cells, K cells, and I cells (15–17). L cells are found in the lower small intestine and colon and secrete

glucagon-like peptide-1 (GLP-1) (18); K cells are found mainly in the upper small intestine and secrete glucose-dependent insulinotropic polypeptide/gastric inhibitory polypeptide (GIP) (16); I cells are found mainly in the upper small intestine and secrete cholecystokinin (CCK) (17). GLP-1 and GIP are the incretins, which are released in response to nutrient ingestion to potentiate insulin secretion from pancreatic β -cells. CCK promotes fat absorption by enhancing pancreatic lipase secretion from pancreatic acinar cells and bile secretion by contracting the gallbladder (19–21). Studies using GIP-knockout mice and CCK-knockout mice have shown that reduction of GIP and CCK secretion alleviates obesity under high-LCT diet-feeding conditions (22, 23). However, the mechanism by which GPR120 signaling in the intestine influences obesity and insulin resistance remains unclear.

In this study, we generated intestine-specific GPR120-knockout (*GPR120^{int-/-}*) mice and investigated the effect on glucose tolerance and secretion of intestinal hormones after single administration of glucose or LCT to clarify the influence of GPR120 signaling on obesity and insulin resistance under high-LCT diet-feeding condition.

MATERIALS AND METHODS

Animals

Male mice with C57BL/6 background were used in all experiments. *GPR120^{int-/-}* mice were generated by crossbreeding floxed GPR120 mice and Villin1 promoter-Cre transgenic (Villin1-Cre Tg) mice (Fig. 1A). Floxed GPR120 mice were used as wild-type (WT) mice. Villin reporter (Villin1-tdTomato) mice, which enabled visualization of intestinal epithelial cells, were generated by crossbreeding Villin1-Cre Tg mice and Ai14 homozygous mice (Supplemental Fig. S1, A and B). Floxed GPR120 mice were generated as reported previously (24). Villin1-Cre Tg mice and Ai14 mice were purchased from Jackson Laboratory (Stock Nos. 004586 and 007908; Bar Harbor, ME). For high-LCT diet studies, 5-wk-old mice received the high-LCT diet with 45% of fat and energy density of 4.7 kcal/g (Cat. No. D12451; Research Diets Inc., New Brunswick, NJ) or the control diet (CD) with 10% of fat and energy density of 3.8 kcal/g (Cat. No. D12450H; Research Diets Inc.) for 15 wk. All mice were maintained in a specific pathogen-free facility under conditions of controlled temperature and 14:10-h light/dark cycle with free access to water and chow unless otherwise stated. Animal care and procedures were approved by Kyoto University Animal Care Committee (KyoMed 19245).

Total Ribonucleic Acid Isolation and RT-PCR

Small intestine (duodenum, jejunum, and ileum), colon, lung, spleen, white adipose tissue (WAT) [(epididymal WAT (eWAT) and inguinal WAT (iWAT)], brown adipose tissue (BAT), liver, and gastrocnemius muscle (skeletal muscle) were taken from WT and *GPR120^{int-/-}* mice for isolation of total RNA. Intraperitoneal macrophages were isolated 3 days after thioglycolate medium (2.0 mL of 3.85%) (Cat. No. 211716; BD, Franklin Lakes, NJ) injection into the abdominal cavity. Total RNAs of adipose tissue were extracted using

RNeasy Lipid Tissue Mini Kit (QIAGEN, Hilden, Germany); total RNAs of the other tissues were extracted using TRIzol reagent (Thermo Fisher Scientific, Waltham, MA). Total RNAs were reverse-transcribed with PrimerScript RT reagent Kit with gDNA Eraser (Takara Bio Inc., Shiga, Japan). SYBR Green PCR Master Mix (Thermo Fisher Scientific) was prepared for the real-time PCR (RT-PCR) run. mRNA expression levels were measured by RT-PCR using the ABI PRISM 7000 Sequence Detection System (Thermo Fisher Scientific). All results are presented using the relative standard curve method normalized to a housekeeping gene (β -actin). Primer pairs designed for evaluation of gene expression are shown in Supplemental Table S1.

Immunohistochemistry

Small intestine, colon, liver, and WAT were fixed by 10% formaldehyde and embedded in paraffin. Some of the sections were stained with hematoxylin and eosin and the other sections were used for immunohistochemistry. The protocol of immunohistochemistry was previously described (25). The sections of the intestine, length of villus, diameter of crypt, and number of chromogranin A, GLP-1, GIP, CCK, or peptide YY (PYY)-expressing cells in 50 villi and crypts were evaluated. The samples in the absence of primary antibodies were included as controls. In immunostained sections of adipose tissue, the mean adipocyte size (surface areas of 15 representative adipocytes per mouse) was analyzed on a single slide glass for each mouse. Anti-chromogranin A antibody (Cat. No. ab15160, RRID: AB_301704, 1:200; Abcam, Cambridge, UK), anti-GLP-1 antibody (Cat. No. Y320, RRID:AB_1964251, 1:1,000; Yanaihara Institute Inc., Fujinomiya, Japan), anti-GIP antibody (Cat. No. PA5-76867, RRID:AB_2720594, 1:100; Thermo Fisher Scientific), anti-CCK antibody (Cat. No. CCK8-MO-167-2, RRID:AB_2572276, 1:200; Frontier Institute Co., Ltd., Ishikari, Japan), anti-PYY antibody (Cat. No. ab22663, RRID:AB_2175186, 1:1,000; Abcam), and anti-RFP antibody (Cat. No. 600-401-379, RRID:AB_2209751, 1:1,000; Rockland Immunochemicals Inc., Pottstown, PA) were used as primary antibodies for the intestine. Anti-perilipin-1 antibody (Cat. No. 9349, RRID: AB_10829911, 1:200; Cell Signaling Technology, Danvers, MA) was used as the primary antibody for adipose tissue. As secondary antibodies, Alexa 546 anti-rabbit (Cat. No. A11035, RRID: AB_2534093, 1:100; Life Technologies Corporation, Carlsbad, CA), Alexa 546 anti-mouse (Cat. No. A11030, RRID: AB_2534089, 1:100; Life Technologies Corporation), Alexa 488 anti-rabbit (Cat. No. A11034, RRID: AB_2576217, 1:100; Life Technologies Corporation), and Alexa 488 anti-mouse (Cat. No. A11029, RRID: AB_2534088, 1:100; Life Technologies Corporation) were used. Images were taken using a fluorescence microscope FSX100 (Olympus Corporation, Tokyo, Japan).

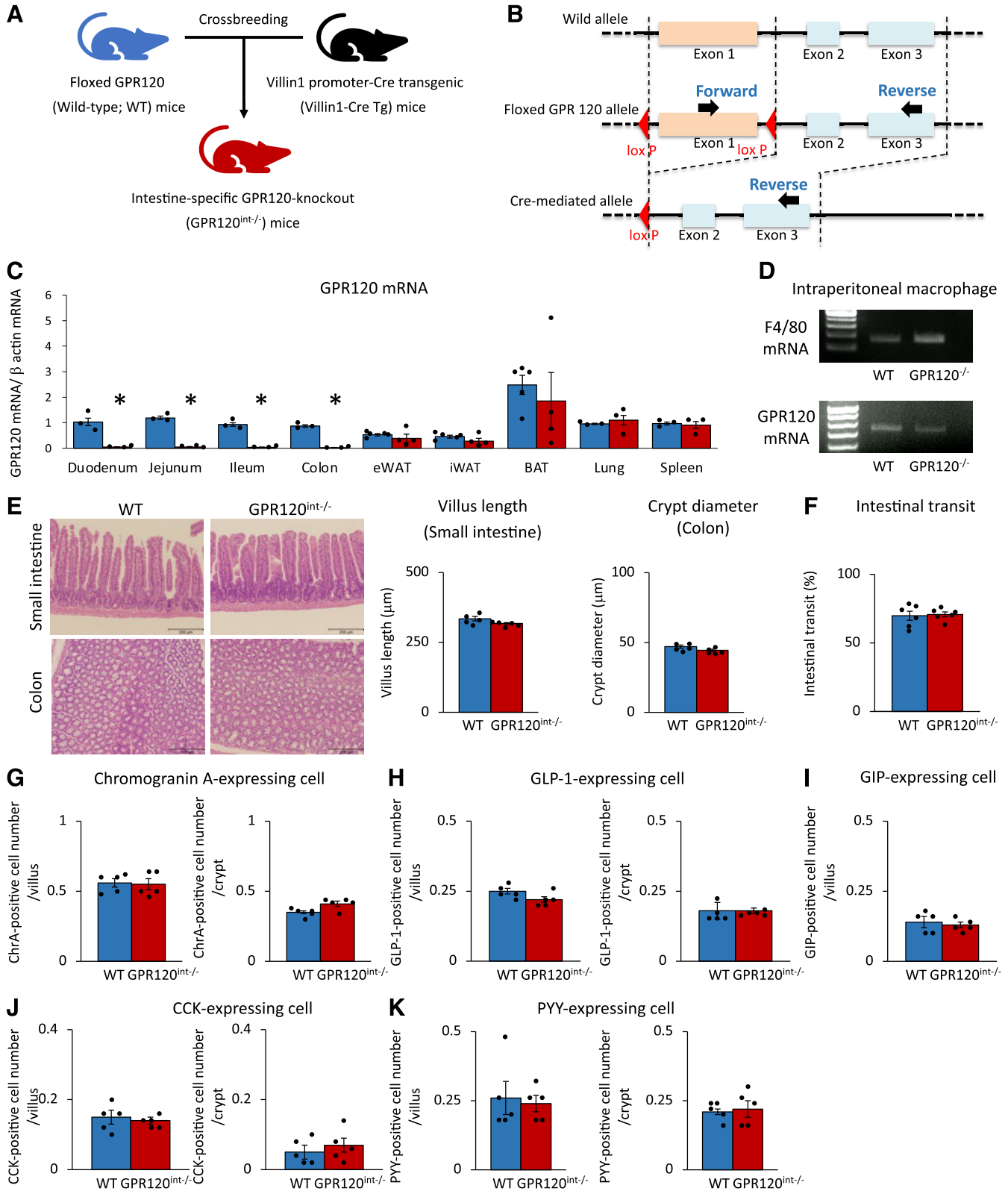
Intestinal Transit

Transit through the stomach and small intestine was measured by administering a nonabsorbed marker containing 10% charcoal suspension in 5% gum Arabic, as previously described (26). The mice were given 0.2 mL of the suspension by oral gavage. Twenty minutes after the oral gavage, the distance from the pylorus to the front of the

charcoal bolus and the ileocecal junction was measured. The transit rate of small intestine was determined as [(distance from pylorus to charcoal front)/(distance from pylorus to ileocecal junction)] × 100 (%).

OGTT and OCTT

Oral glucose tolerance tests (OGTTs) and oral corn oil tolerance tests (OCTTs) were performed in 10- to 15-wk-old



mice. After a 16-h fasting period, mice were administered glucose (6 g/kg body wt for GLP-1 measurement and 2 g/kg body wt for others) by oral gavage for OGTTs; corn oil (10 mL/kg body wt) was administered by oral gavage for OCTTs (27). Subsequently, 45 μ L blood samples were collected via tail vein at 0 (15 min for OGTTs), 30, 60, and 120 min. Blood glucose levels were measured using the glucose oxidase method (Sanwa Kagaku Kenkyusho Co., Ltd., Nagoya, Japan).

Enzyme-Linked Immunosorbent Assays

Concentrations of plasma insulin, total GIP, total GLP-1, PYY, CCK, interleukin (IL)-6, and TNF- α were measured using ELISA kits for insulin (Cat. No. AKRIN-031; FUJIFILM Wako Shibayagi Corporation, Shibukawa, Japan), total GIP (Cat. No. EZRMGIP-55K; Merck, Billerica, MA), total GLP-1 (Cat. No. K1503PD-1; Meso Scale Discovery, Rockville, MD), PYY (Cat. No. YK081; Yanaihara Institute Inc.), CCK (Cat. No. FEK-069-04; Phoenix Pharmaceuticals Inc., Burlingame, CA), IL-6 (Cat. No. RSD-M6000B-1; R&D Systems, Minneapolis, MN), and TNF- α (Cat. No. AKMTNFA-011; FUJIFILM Wako Shibayagi Corporation), respectively.

Measurement of Lipase Activity and Gallbladder Contraction during OGTT and OCTT

After 16-h fasting, the mice were administered glucose (2 g/kg body wt) by oral gavage for OGTTs; corn oil (10 mL/kg body wt) was administered by oral gavage for OCTTs. In addition, the jejunum and gallbladder were removed 15 min after oral glucose administration and 30 min after oral corn oil administration. Small intestine contents were collected from jejunum and centrifuged at 15,000 rpm for 10 min at 4°C. A water layer was used for the measurement of intestinal lipase activity by the BALB-DTNB method (SB Bioscience, Tokyo, Japan) (28). Bile in the gallbladder was collected using a 29 G syringe (Terumo, Tokyo, Japan); bile volume was assessed by the volume of bile remaining in the gallbladder.

Measurement of Lipase Activity and Gallbladder Contraction Using CCK Agonist

OCTT was performed in 16-h fasted mice immediately after injection of CCK agonist (200 ng/kg body wt) via tail vein. [Thr28, Nle31]-CCK (Cat. No. AS-22944; AnaSpec, Inc., Fremont, CA) was used as a CCK agonist. The jejunum and gallbladder were removed 30 min after oral corn oil administration. Small intestine contents were collected from jejunum and centrifuged at 15,000 rpm for 10 min at 4°C. A water layer was used for the measurement of intestinal lipase activity by the BALB-DTNB method (SB Bioscience, Tokyo,

Japan) (28). Bile in the gallbladder was collected using a 29 G syringe (Terumo, Tokyo, Japan); bile volume was assessed by the volume of bile remaining in the gallbladder.

Insulin Tolerance Test

The mice were fasted for 4 h before the start of the experiment. Blood samples were drawn from the tail vein at the following time intervals: 0 min (fasting levels) and 30, 60, 90, and 120 min after intraperitoneal administration of human insulin (0.5 units/kg body wt) (Eli Lilly and Co., Indianapolis, IN) (27). Blood glucose levels were measured by the glucose oxidase method (Sanwa Kagaku Kenkyusho). Results were calculated with blood glucose levels at 0 min being considered 100%.

Hepatic Lipid Parameters

Extraction of hepatic lipids was done as described previously (29); triglyceride (TG) levels were evaluated using an enzymatic assay kit (Sekisui Medical Co., Ltd., Tokyo, Japan). TG content in liver was measured as per gram of liver tissue weight.

Western Blotting

For insulin stimulation, human regular insulin (2.0 units/kg body wt) was administered through the inferior vena cava of mice anesthetized with isoflurane. Three minutes later, samples of liver, eWAT, iWAT, and gastrocnemius muscle (skeletal muscle) were dissected and immediately frozen in liquid nitrogen. Frozen tissue extracts were homogenized in cold radioimmunoprecipitation assay buffer composed of 50 mmol/L Tris-HCl (pH 7.4), 150 mmol/L NaCl, 1% NP-40, 0.1% SDS, 1 mmol/L EDTA, phosphatase inhibitor cocktail (Sigma Aldrich, St. Louis, MO), and protease inhibitor cocktail (Roche, Basel, Switzerland) and centrifuged at 11,000 rpm at 4°C for 5 min. Equal amounts of proteins were subjected to immunoblot analysis (30). Anti-Akt antibody (Cat. No. 9272, RRID: AB_329827, 1:1,000; Cell Signaling Technology) and anti-phosphorylated-Akt (Ser473) antibody (Cat. No. 9271, RRID: AB_329825, 1:1,000; Cell Signaling Technology) were used as primary antibodies. Anti-Rabbit IgG (Cat. No. NA934, RRID: AB_772206, 1:2,000; GE Healthcare, Chicago, IL) was used as a secondary antibody.

Statistical Analysis

The results are shown as means \pm standard error of the mean (SEM). Statistical significance was determined using Student's *t* test and Mann-Whitney *U* test. Statistical analyses were performed using the JMP Pro version 16.1.0 (SAS Institute, Cary, NC). *P* values < 0.05 were considered statistically significant.

Figure 1. Intestinal morphology and enteroendocrine cells number in *GPR120*^{int-/-} mice. WT mice and *GPR120*^{int-/-} mice are represented by blue bars and red bars, respectively. *A*: crossbreeding of floxed *GPR120* mice and Villin1 promoter-Cre transgenic (Villin1-Cre Tg) mice was used to generate *GPR120*^{int-/-} mice. *B*: schematic representation of the floxed *GPR120* gene using Cre-loxP-mediated recombination. *C*: RT-PCR analysis of *GPR120* mRNA expression in duodenum, jejunum, ileum, colon, epididymal white adipose tissue (eWAT), inguinal white adipose tissue (iWAT), brown adipose tissue (BAT), lung, and spleen (*n* = 3–5). *D*: RT-PCR analysis of *GPR120* mRNA expression in intraperitoneal macrophages. F4/80 mRNA is used as a macrophage marker. *E*: villus length of small intestine and crypt diameter of colon (*n* = 5). *F*: intestinal transit after oral administration of nonabsorbed marker (10% charcoal suspension in 5% gum Arabic). *G–K*: number of chromogranin A (G), GLP-1 (H), GIP (I), CCK (J), and PYY-expressing cells in villus of small intestine and crypt of colon (*n* = 5) (K). **P* < 0.05 vs. WT. WT, wild-type.

RESULTS

Generation of *GPR120*^{int-/-} Mice

Prior to generation of *GPR120*^{int-/-} mice from Villin1-Cre Tg mice, we investigated Villin expression in the intestine using Villin1-tdTomato mice (Supplemental Fig. S1A). Villin was found to be expressed in all intestinal epithelial cells of the small intestine and colon (Supplemental Fig. S1, B and D). Villin was also expressed in chromogranin A, CCK, GLP-1, GIP, and PYY-expressing cells (Supplemental Fig. S1, C and D). Cre-mediated recombination was found to occur in exon 1 of *GPR120* by the presence of both the floxed *GPR120* gene and Villin1-Cre transgene in *GPR120*^{int-/-} mice (Fig. 1B). Expression of *GPR120* mRNA in small intestine, colon, eWAT, iWAT, BAT, lung, and spleen was determined by RT-PCR (Fig. 1C). When the specific primers were used for amplification of exon 1 and exon 3 (Fig. 1B), the expression levels of *GPR120* mRNA were more than 90% lower in small intestine and colon in *GPR120*^{int-/-} mice than those in WT mice. However, the expression levels in eWAT, iWAT, BAT, lung, and spleen were not significantly different between WT and *GPR120*^{int-/-} mice (Fig. 1C). Because the expression levels of *GPR120* mRNA were very low in intraperitoneal macrophages, we analyzed the bands of PCR product by electrophoresis; a band was clearly detected in macrophages of *GPR120*^{int-/-} mice as well as in WT mice (Fig. 1D).

Subsequently, we evaluated intestinal morphology, intestinal transit, and number of enteroendocrine cells in the small intestine and colon. The length of villus, diameter of crypt, and intestinal transit were not significantly different between WT and *GPR120*^{int-/-} mice (Fig. 1, E and F). The numbers of chromogranin A (Fig. 1G), GLP-1 (Fig. 1H), GIP (Fig. 1I), CCK (Fig. 1J), and PYY (Fig. 1K)-expressing cells did not differ between the two groups.

Secretion of Intestinal Hormones and CCK Action after Single Administration of Glucose or Corn Oil in *GPR120*^{int-/-} Mice

Blood glucose, insulin, GIP, GLP-1, and PYY levels were measured during OGTTs and OCTTs. In the OGTTs and OCTTs, blood glucose, insulin, GLP-1, and PYY levels did not differ between WT and *GPR120*^{int-/-} mice (Fig. 2, A-F), except for the single change in blood glucose levels at 120 min during OGTT (Fig. 2A). Area under the curve of (AUC) glucose did not significantly differ between the two groups (Fig. 2, A and B). In OGTT, total GIP levels did not differ between the two groups (Fig. 2C). On the other hand, total GIP levels after administration of corn oil were significantly lower in *GPR120*^{int-/-} mice than those in WT mice (Fig. 2D). Because available antibody in the ELISA kit for measuring CCK is crossreactive with gastrin, CCK levels also were found not to be significantly different between WT and *GPR120*^{int-/-} mice (data not shown). To evaluate CCK action, remaining bile volume in the gallbladder and intestinal lipase activity during OGTT and OCTT was measured. In OGTT, bile volume and intestinal lipase activity did not differ between WT and *GPR120*^{int-/-} mice (Fig. 2, G and I). In contrast, bile volume was significantly larger, and intestinal lipase activity was significantly lower in *GPR120*^{int-/-} mice than those in WT mice after single oral administration of corn oil (Fig. 2, H and J).

CCK agonist completely restored CCK action (gallbladder contraction and intestinal lipase activity) in *GPR120*^{int-/-} mice (Supplemental Fig. S2, A and B). Moreover, CCK agonist restored GIP secretion in *GPR120*^{int-/-} mice (Supplemental Fig. S2C). These results suggest that inhibition of *GPR120* signaling in intestine reduces LCT-induced GIP secretion and CCK action but not LCT-induced GLP-1 or PYY secretion.

Expression Levels of *GPR120* mRNA, Body Weight, Insulin Sensitivity, and Glucose Tolerance in high-LCT Diet-Fed *GPR120*^{int-/-} Mice

The expression levels of *GPR120* mRNA under high LCT diet in WT mice were lower in eWAT and iWAT and higher in BAT and spleen than those under CD diet in WT mice (Supplemental Fig. S3A). On the other hand, the expression levels in intestine did not differ between CFD diet-fed WT and high-LCT diet-fed WT mice. *GPR120* mRNA was clearly detected in macrophages of both mice (Supplemental Fig. S3B).

Body weight did not differ between CD-fed WT and *GPR120*^{int-/-} mice (Supplemental Fig. S4A). After 15 wk of CD feeding, ITT and OGTT data showed that insulin sensitivity and glucose tolerance were similar between the two groups of mice (Supplemental Fig. S4, B-D).

Under high-LCT diet condition, body weight was mildly but significantly reduced in *GPR120*^{int-/-} mice compared with that in WT mice (Fig. 3A). After 15 wk of high-LCT diet feeding, ITT data showed that insulin sensitivity was higher in *GPR120*^{int-/-} mice than that in WT mice (Fig. 3B). In OGTT, although blood glucose levels did not differ, insulin levels at 30 min and AUC-insulin were significantly lower in *GPR120*^{int-/-} mice than those in WT mice (Fig. 3, C and D).

We then measured the weight of liver, eWAT, perirenal WAT (pWAT), iWAT, and skeletal muscle of high-LCT diet-fed WT and *GPR120*^{int-/-} mice. The weight of liver, eWAT, and pWAT were significantly lower in *GPR120*^{int-/-} mice than those in WT mice (Fig. 3E).

By histological analysis of the liver, lipid droplets were found to be reduced in *GPR120*^{int-/-} mice (Fig. 3F and Supplemental Fig. S5A). Adipocyte size was also significantly smaller in *GPR120*^{int-/-} mice than those in WT mice (Fig. 3F and Supplemental Fig. S5B). TG content in liver was significantly lower in *GPR120*^{int-/-} mice than that in WT mice (Fig. 3G).

Akt Phosphorylation in Liver, WAT, and Skeletal Muscle after Insulin Treatment

In the in vivo study using *GPR120*^{int-/-} mice, inhibition of *GPR120* signaling in the intestine was shown to ameliorate insulin resistance and fatty liver under high-LCT diet-feeding conditions. We then evaluated phosphorylation (Ser473) of serine/threonine kinase Akt in liver, eWAT, iWAT, and skeletal muscle. Insulin treatment increased Akt phosphorylation in all four tissues (Fig. 4, A-D). The ratios of phosphorylated Akt to total Akt in liver, eWAT, and iWAT were significantly higher in *GPR120*^{int-/-} mice than those in WT mice (Fig. 4, A-C), but the ratio of skeletal muscle did not differ between the two groups (Fig. 4D).

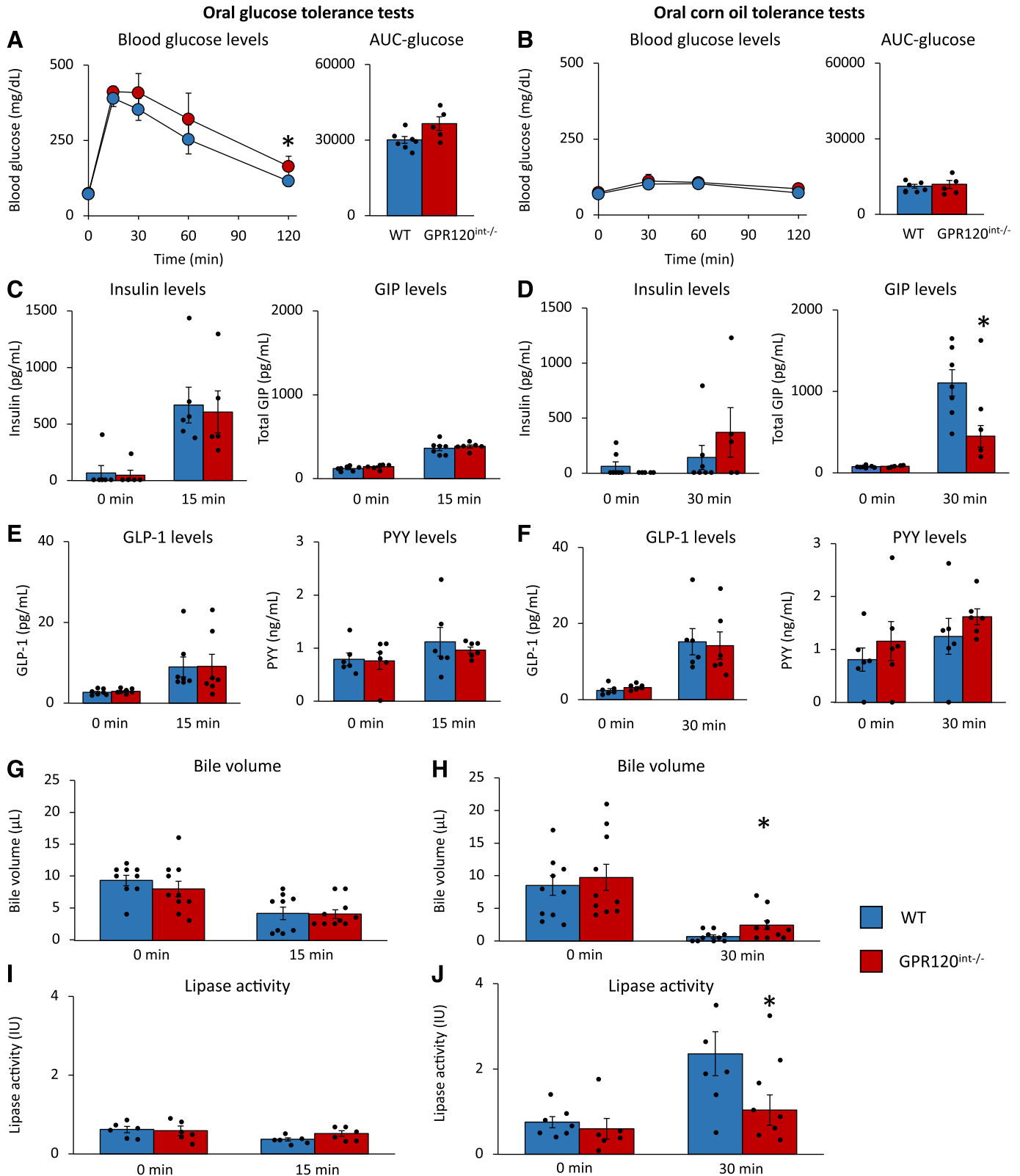


Figure 2. OGTTs and OCTTs in WT and *GPR120*^{int-/} mice. WT mice are represented by blue bars and blue circles. *GPR120*^{int-/} mice are represented by red bars and red circles. A–F: glucose (A), insulin, GIP, (C), GLP-1, and PYY levels during oral glucose tolerance test (OGTT) (E). Glucose (B), insulin, GIP (D) GLP-1, and PYY levels during oral corn oil tolerance test (OCTT) (*n* = 5–7) (F). AUC indicates area under the curve. G–J: remaining bile volume in the gallbladder (*n* = 9 or 10) (G) and lipase activity in the intestinal contents during OGTT (*n* = 6) (I). Remaining bile volume in the gallbladder (*n* = 10) (H) and lipase activity in the intestinal contents during OCTT (*n* = 6–8) (J). **P* < 0.05 vs. WT. WT, wild-type.

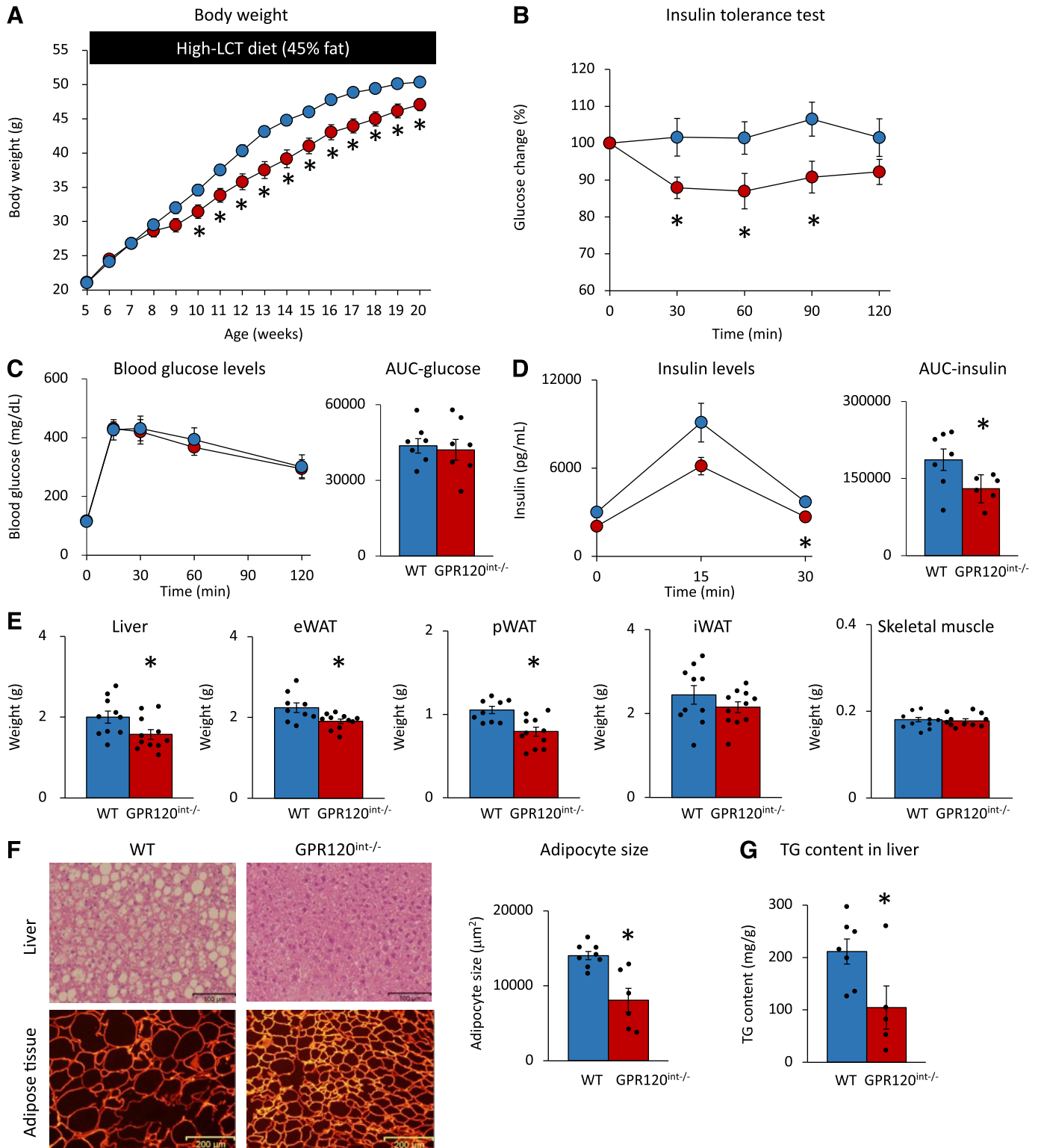


Figure 3. Phenotype of high-LCT diet-fed *GPR120*^{int-/-} mice. WT mice are represented by blue bars and blue circles. *GPR120*^{int-/-} mice are represented by red bars and red circles. Body weight changes ($n = 7$) (A). Insulin tolerance test after 15 wk of high-LCT diet ($n = 7$) (B). C and D: glucose (C) and insulin levels during oral glucose tolerance test ($n = 6$ or 7) (D). AUC indicates area under the curve. Weight of liver, epididymal white adipose tissue (eWAT), perirenal white adipose tissue (pWAT), inguinal white adipose tissue (iWAT), and skeletal muscle ($n = 9$ – 11) (E). F: representative histological images of liver (hematoxylin and eosin staining) (left) and eWAT (immunohistochemical staining using anti-perilipin-1 antibody) in the mice after 15 wk of high-LCT diet feeding (right) Adipocyte size in eWAT ($n = 6$ – 8). G: triglyceride (TG) content in liver ($n = 5$ – 7) * $P < 0.05$ vs. WT. AUC, area of the curve; LCT, long-chain triglyceride; WT, wild-type.

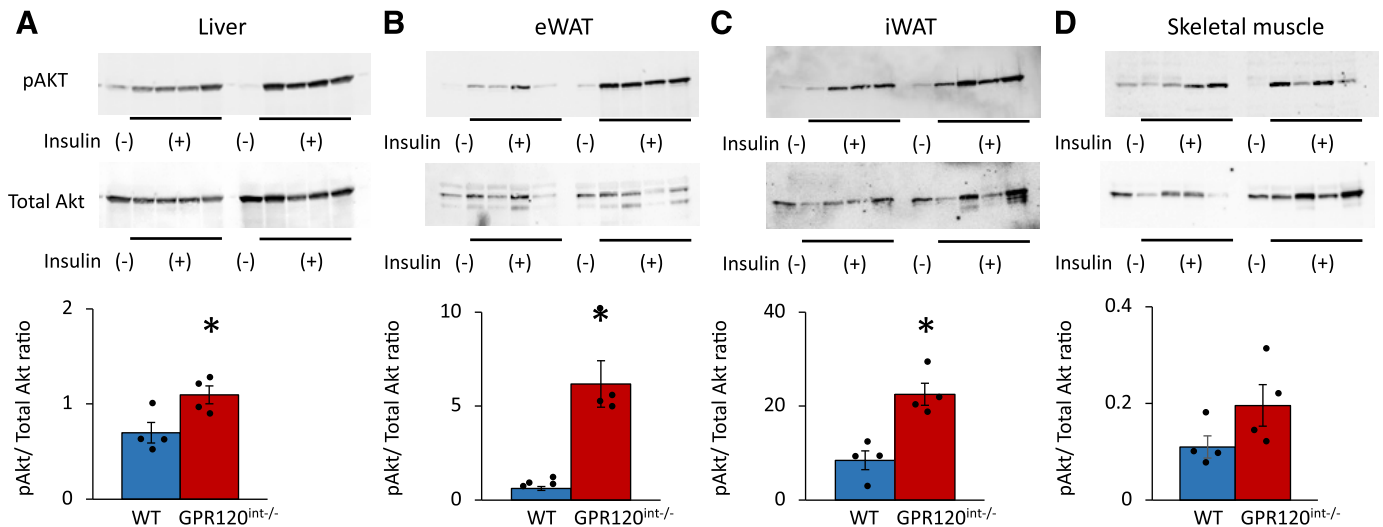


Figure 4. Western blot analysis of Akt (Ser473) phosphorylation. Total Akt and phosphorylated Akt (pAkt) proteins in liver (A), epididymal white adipose tissue (eWAT) (B), inguinal white adipose tissue (iWAT) (C), and skeletal muscle of WT and *GPR120^{int-/-}* mice after 15 wk of high-LCT diet feeding (D). Bar charts show the ratios of pAkt/Total Akt 3 min after administration of insulin ($n = 4$). * $P < 0.05$ vs. WT. LCT, long-chain triglyceride; WT, wild-type.

Gene Expression of Molecules Associated with Insulin Signaling in Liver, WAT, and Skeletal Muscle

GPR120 agonist lowers expression of proinflammatory genes in eWAT such as IL-6, TNF- α , monocyte chemoattractant protein 1 (MCP1), and IL-1 β , which is attenuated in global GPR120-knockout mice (13). We, therefore, investigated the influence of intestinal GPR120 signaling on the inflammatory cytokines that have been reported to be reduced by GPR120 signaling in eWAT. The expression levels of IL-6 mRNA, MCP1 mRNA, and IL-1 β mRNA were significantly lower in eWAT of *GPR120^{int-/-}* mice on a high-LCT diet than those of WT mice. Although there was not a significant difference, the expression levels of TNF- α mRNA tended to be lower in eWAT of *GPR120^{int-/-}* mice compared with those of WT mice (Fig. 5A). Plasma IL-6 levels were significantly lower in *GPR120^{int-/-}* mice than those in WT mice (Fig. 5B), whereas plasma TNF- α levels were not detectable, being under the limit of sensitivity of the assay (data not shown).

We then focused on factors that mediate inflammatory cytokines and improved insulin sensitivity in *GPR120^{int-/-}* mice under a high-LCT diet. Suppressor of cytokine signaling 1 (SOCS1) and SOCS3 are activated by inflammatory cytokines such as IL-6 and inhibit insulin signaling by competing for insulin receptor substrate binding sites on the insulin receptor (31–33). SOCS1 and SOCS3 are also involved in hepatic steatosis via sterol regulatory element-binding protein-1c (SREBP-1c) (33). The expression levels of SOCS3 mRNA were significantly lower in the liver, eWAT, and iWAT of *GPR120^{int-/-}* mice than those in WT mice, but the expression levels of SOCS1 mRNA were not significantly different between the two groups (Fig. 5, C–E). In skeletal muscle, the expression levels of SOCS1 mRNA and SOCS3 mRNA did not differ between the two groups (Fig. 5F). SREBP-1c activates stearoyl-CoA desaturase 1 (SCD1) and acetyl-CoA carboxylase (ACC), which are rate-limiting enzymes for fatty acid synthesis that induce steatosis and fibrosis in the liver (34). The expression levels of SREBP-1c mRNA, SCD1 mRNA,

and ACC mRNA were reduced in the liver of *GPR120^{int-/-}* mice (Fig. 5G).

DISCUSSION

In this study, we generated *GPR120^{int-/-}* mice to investigate the metabolic effects of GPR120 in the intestine. Under long-term feeding of a high-LCT diet, inhibition of GPR120 signaling in the intestine mitigated obesity, insulin resistance, and hepatic steatosis.

According to previous reports, global inhibition of GPR120 signaling exacerbates obesity and insulin resistance on a high-LCT diet (10, 11, 13) while GPR120 agonist ameliorates insulin resistance by lowering inflammatory cytokine production from adipose tissue and macrophages (10, 13). In this study, *GPR120^{int-/-}* mice were found to exhibit a mild reduction of body weight and substantial improvement of insulin resistance without a change in glucose tolerance. These findings suggested that while GPR120 signaling in adipose tissue and macrophages inhibits exacerbation of obesity and insulin resistance by negatively regulating inflammation, intestinal GPR120 signaling promotes obesity and insulin resistance on a high-LCT diet. GPR120 is highly expressed in enteroendocrine cells and is reported to be associated with the secretion of intestinal hormones such as GLP-1, PYY, CCK, and GIP (15–18, 34, 35). GLP-1 and PYY are well-known to reduce body weight via suppression of food intake while CCK and GIP in concert have a role in digestion, absorption, and storage of LCT. In this study, *GPR120^{int-/-}* mice showed reduced GIP secretion and CCK action without a change in GLP-1 or PYY secretion after a single administration of LCT.

Although these results showed that inhibition of GPR120 in the intestine reduces body weight by altering secretion of intestinal hormones such as GIP and CCK, other hormones not evaluated in this study might also be involved. Although bile acids are reported to stimulate GLP-1 secretion (36, 37), reduced gallbladder emptying and lipase activity in *GPR120^{int-/-}* mice did not affect GLP-1 levels.

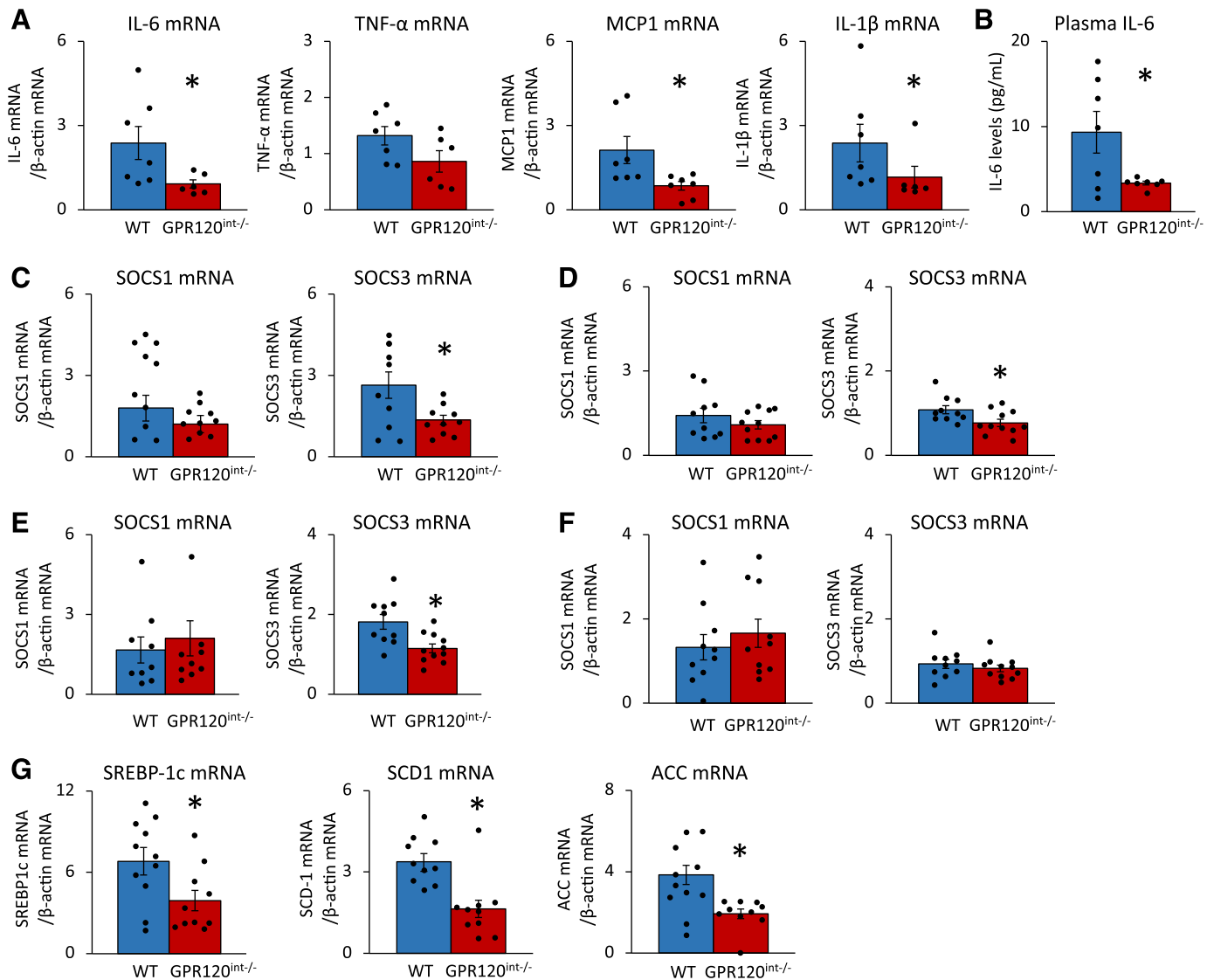


Figure 5. Inflammatory cytokines and molecules associated with insulin resistance. **A:** mRNA expression levels of IL-6, TNF- α , MCP1, and IL-1 β in epididymal white adipose tissue (eWAT) of WT and *GPR120*^{int-/} mice after 15 wk of high-LCT diet feeding ($n = 6$ or 7). **B:** plasma IL-6 levels ($n = 7$). **C–F:** mRNA expression levels of SOCS1 and SOCS3 in liver (**C**), eWAT (**D**), inguinal white adipose tissue (iWAT) (**E**), and skeletal muscle of WT and *GPR120*^{int-/} mice after 15 wk of high-LCT diet feeding ($n = 9–11$) (**F**). **G:** mRNA expression levels of SREBP-1c, SCD1, and ACC in liver ($n = 10$ or 11). * $P < 0.05$ vs. WT. ACC, acetyl-CoA carboxylase; LCT, long-chain triglyceride; MCP1, monocyte chemoattractant protein 1; SCD1, activates stearyl-CoA desaturase 1; SREBP-1c, sterol regulatory element-binding protein-1c; WT, wild-type.

Reduced gallbladder emptying and lipase activity could potentially increase the interaction of lipids with the more distal gut regions, allowing GLP-1 to be stimulated more effectively, which could overcome the reduction of bile-evoked GLP-1 release. Female mice were not used to avoid the influence of estradiol in this study. Further study is required to assess sex-based differences in the metabolic phenotype of *GPR120*^{int-/} mice.

In this study, inhibition of GPR120 signaling in intestine was found to reduce the weight of liver and visceral WAT and markedly enhance Akt phosphorylation in visceral WAT under high-fat diet feeding conditions. Earlier studies reported that insulin and GIP signaling in adipose tissue are involved in fat accumulation in adipose tissue and liver (38, 39). High-LCT diet feeding is known to strongly stimulate

GIP secretion from K cells (40, 41) while inhibition of GIP signaling or GIP secretion ameliorates obesity on a high-LCT diet, which is accompanied by an increase in fat oxidation and energy expenditure (22, 42). In addition, GIP signaling in adipose tissue is associated with insulin resistance and hepatic steatosis via IL-6 and SOCS signaling (38). Moreover, visceral WAT is involved in the gastrointestinal tract and liver via lymph ducts and the portal vein, respectively; venous blood of subcutaneous WAT is drained through systemic veins (43). It is thought that inhibition of GPR120 signaling in intestine has a large influence on visceral WAT, especially considering the strong association with the gastrointestinal tract both anatomically and metabolically. On the other hand, Akt phosphorylation in skeletal muscle did not differ between the two groups. Further study is necessary to

elucidate the mechanism by which Akt phosphorylation is increased in liver and adipose tissue of *GPR120^{int-/-}* mice without significant change in skeletal muscle.

Key molecules affected by inhibition of intestinal GPR120 signaling are potentially associated with lessening of insulin resistance and hepatic steatosis on high-LCT diet. Obesity is strongly associated with mRNA expression of inflammatory cytokines such as IL-6 from macrophages and adipocytes (44). Increased circulating levels of IL-6 promotes expression of SOCS1 and SOCS3 in liver, adipose tissue, and skeletal muscle, which induces insulin resistance through the inhibition of insulin receptor signaling by SOCS1 and SOCS3 (45, 46). In addition, SOCS1 and SOCS3 bind to the promoter of the SREBP-1c gene in liver, which can lead to hepatic steatosis (33). In this study, the mRNA expression levels of inflammatory cytokines in adipose tissue and plasma IL-6 levels were found to be reduced in *GPR120^{int-/-}* mice, unlike those in global GPR120-deficient mice found in a previous study (13). Moreover, the mRNA expression levels of SOCS3 but not SOCS1 were reduced in the liver and adipose tissue, and those of SREBP-1c, SCD1, and ACC were reduced in the liver of *GPR120^{int-/-}* mice. Thus, not only inhibition of intestinal GPR120 signaling but also preservation of the anti-inflammatory effect of GPR120 in adipose tissue and macrophages may be involved in the inflammatory cytokine levels to improve insulin resistance and hepatic steatosis via reduction of SOCS3 signaling.

Unlike single corn oil administration, single administration of glucose did not affect GIP secretion or CCK action in *GPR120^{int-/-}* mice. Inhibition of intestinal GPR120 signaling also did not alter body weight, insulin sensitivity, or glucose tolerance on the CD diet. Because GPR120 is a specific receptor of LCT, these findings indicate that GPR120 does not play a role in intestinal hormone secretion, body weight, or insulin sensitivity under carbohydrate-rich CD diet feeding.

With regard to possible drug discovery and development, molecules that inhibit GPR120 signaling in intestine might be expected to mitigate insulin resistance and hepatic steatosis. We previously reported that medium-chain triglycerides (MCTs) ameliorate obesity on high-LCT diet through inhibition of GPR120 signaling in intestine (47, 48). As MCTs are localized in intestine and liver, molecules with similar structures might selectively inhibit intestinal GPR120. Such molecules have not been developed partly because the three-dimensional structure of GPR120 has not been revealed. Thus, it is desirable to determine the detailed structure of GPR120 to identify molecules with high affinity to GPR120 in intestine.

In conclusion, our results indicate that GPR120 in intestine enhances LCT-induced GIP secretion and CCK action and exacerbates insulin resistance and hepatic steatosis under high-LCT diet feeding conditions. Moreover, inhibition of GPR120 signaling in intestine slightly ameliorates obesity while substantially improving insulin resistance and hepatic steatosis in liver and WAT, which is accompanied by increased Akt phosphorylation and reduced expression levels of SOCS3. Molecules that inhibit intestinal GPR120 signaling might therefore contribute to treatment of lifestyle diseases such as obesity, diabetes mellitus, and hepatic steatosis.

DATA AVAILABILITY

Data will be made available upon reasonable request.

SUPPLEMENTAL DATA

Supplemental Table S1: <https://doi.org/10.6084/m9.figshare.21687518>.

Supplemental Figs. S1–S5: <https://doi.org/10.6084/m9.figshare.21687491>.

ACKNOWLEDGMENTS

We thank Dr. Erina Joo, Dr. Toshihiro Nakamura, and Dr. Junji Fujikura for technical suggestions.

GRANTS

This study was supported by grants from the Ministry of Education, Culture, Sports, Science and Technology (MEXT), Japan Society for the Promotion of Science (JSPS, Grant Nos. 22K08668, 21J13647, and 20H03731), Ministry of Health, Labour, and Welfare, Ministry of Agriculture, Forestry and Fisheries, Japan Diabetes Foundation, Japan Association for Diabetes Education and Care, Merck Sharp & Dohme (MSD) Life Science Foundation, Public Interest Incorporated Foundation, and Suzuken Memorial Foundation.

DISCLOSURES

N. I. received joint research grants from Daiichi Sankyo Co., Ltd., Terumo Co., Ltd., and Drawbridge, Inc.; N.I. received speaker honoraria from Kowa Pharmaceutical Co., Ltd.; MSD, Astellas Pharma Inc., Novo Nordisk Pharma Ltd., Ono Pharmaceutical Co., Ltd., Nippon Boehringer Ingelheim Co., Ltd., Takeda Pharmaceutical Co., Ltd., and Mitsubishi Tanabe Pharma Co., Ltd.; N.I. received scholarship grants from Kissei Pharmaceutical Co., Ltd., Sanofi, Daiichi Sankyo Co., Ltd., Mitsubishi Tanabe Pharma Co., Ltd., Takeda Pharmaceutical Co., Ltd., Japan Tobacco Inc., Kyowa Kirin Co., Ltd., Sumitomo Dainippon Pharma Co., Ltd., Astellas Pharma Inc., MSD, Eli Lilly Japan, Ono Pharmaceutical Co. Ltd., Sanwa Kagaku Kenkyusho Co. Ltd., Nippon Boehringer Ingelheim Co., Ltd., Novo Nordisk Pharma Ltd., Novartis Pharma K.K., Teijin Pharma Ltd., and Life Scan Japan Inc. N. H. received scholarship grants from Mitsubishi Tanabe Pharma Co., Ltd., Ono Pharmaceutical Co. Ltd., and Sanofi K.K.

AUTHOR CONTRIBUTIONS

T.Y., N.I., and N.H. conceived and designed research; T.Y., N.H., T.H., E.I.-O., Y.M., N.W., and S.K. performed experiments; T.Y. and N.H. analyzed data; T.Y., N.H., A.I., S.Y., A.H., and N.I., interpreted results of experiments; T.Y. and N.H. prepared figures; T.Y. and N.H. drafted manuscript; T.Y., N.H., and N.I. edited and revised manuscript; T.Y., N.H., T.H., A.I., E.I.-O., Y.M., N.W., S.K., S.Y., A.H., and N.I. approved final version of manuscript.

REFERENCES

1. **Morgen CS, Sørensen T.** Obesity: global trends in the prevalence of overweight and obesity. *Nat Rev Endocrinol* 10: 513–514, 2014. doi:10.1038/nrendo.2014.124.
2. **Bray GA, Paeratakul S, Popkin BM.** Dietary fat and obesity: a review of animal, clinical and epidemiological studies. *Physiol Behav* 83: 549–555, 2004. doi:10.1016/j.physbeh.2004.08.039.
3. **Kahn BB, Flier JS.** Obesity and insulin resistance. *J Clin Invest* 106: 473–481, 2000. doi:10.1172/JCI10842.

4. Lemieux I, Pascot A, Couillard C, Lamarche B, Tchernof A, Alméras N, Bergeron J, Gaudet D, Tremblay G, Prud'homme D, Nadeau A, Després JP. Hypertriglyceridemic waist: a marker of the atherogenic metabolic triad (hyperinsulinemia; hyperapoprotein B; small, dense LDL) in men? *Circulation* 102: 179–184, 2000. doi:10.1161/01.cir.102.2.179.
5. Petrie JR, Guzik TJ, Touyz RM. Diabetes, hypertension, and cardiovascular disease: clinical insights and vascular mechanisms. *Can J Cardiol* 34: 575–584, 2018. doi:10.1016/j.cjca.2017.12.005.
6. Zhao YF. Free fatty acid receptors in the endocrine regulation of glucose metabolism: insight from gastrointestinal-pancreatic-adipose interactions. *Front Endocrinol (Lausanne)* 13: 956277, 2022. doi:10.3389/fendo.2022.956277.
7. Kimura I, Ichimura A, Ohue-Kitano R, Igarashi M. Free fatty acid receptors in health and disease. *Physiol Rev* 100: 171–210, 2020. doi:10.1152/physrev.00041.2018.
8. Fredriksson R, Höglund PJ, Gloriam DE, Lagerström MC, Schiöth HB. Seven evolutionarily conserved human rhodopsin G protein-coupled receptors lacking close relatives. *FEBS Lett* 20: 381–388, 2003. doi:10.1016/s0014-5793(03)01196-7.
9. Hirasawa A, Tsumaya K, Awaji T, Katsuma S, Adachi T, Yamada M, Sugimoto Y, Miyazaki S, Tsujimoto G. Free fatty acids regulate gut incretin glucagon-like peptide-1 secretion through GPR120. *Nat Med* 11: 90–94, 2005. doi:10.1038/nm1168.
10. Oh DY, Talukdar S, Bae EJ, Imamura T, Morinaga H, Fan WQ, Li P, Lu WJ, Watkins SM, Olefsky JM. GPR120 is an omega-3 fatty acid receptor mediating potent anti-inflammatory and insulin-sensitizing effects. *Cell* 142: 687–698, 2010. doi:10.1016/j.cell.2010.07.041.
11. Ichimura A, Hirasawa A, Poulain OG, Bonnefond A, Hara T, Yengo L et al. Dysfunction of lipid sensor GPR120 leads to obesity in both mouse and human. *Nature* 483: 350–354, 2012. doi:10.1038/nature10798.
12. Talukdar S, Olefsky JM, Osborn O. Targeting GPR120 and other fatty acid-sensing GPCRs ameliorates insulin resistance and inflammatory diseases. *Trends Pharmacol Sci* 32: 543–550, 2011. doi:10.1016/j.tips.2011.04.004.
13. Oh DY, Walenta E, Akiyama TE, Lagakos WS, Lackey D, Pessentheiner AR, Sasik R, Hah N, Chi TJ, Cox JM, Powels MA, Salvo JD, Sinz C, Watkins SM, Armando AM, Chung H, Evans RM, Quehenberger O, McNelis J, Bogner-Strauss JG, Olefsky JM. A Gpr120-selective agonist improves insulin resistance and chronic inflammation in obese mice. *Nat Med* 20: 942–947, 2014. doi:10.1038/nm.3614.
14. Paschoal VA, Walenta E, Talukdar S, Pessentheiner AR, Osborn O, Hah N, Chi TJ, Tye GL, Armando AM, Evans RM, Chi NW, Quehenberger O, Olefsky JM, Oh DY. Positive reinforcing mechanisms between GPR120 and PPAR γ modulate insulin sensitivity. *Cell Metab* 31: 1173–1188.e5, 2020. doi:10.1016/j.cmet.2020.04.020.
15. Reimann F, Habib AM, Tolhurst G, Parker HE, Rogers GJ, Gribble FM. Glucose sensing in L cells: a primary cell study. *Cell Metab* 8: 532–539, 2008. doi:10.1016/j.cmet.2008.11.002.
16. Iwasaki K, Harada N, Sasaki K, Yamane S, Iida K, Suzuki K, Hamasaki A, Nasteska D, Shibue K, Joo E, Harada T, Hashimoto T, Asakawa Y, Hirasawa A, Inagaki N. Free fatty acid receptor GPR120 is highly expressed in enteroendocrine K cells of the upper small intestine and has a critical role in GIP secretion after fat ingestion. *Endocrinology* 156: 837–846, 2015. doi:10.1210/en.2014.1653.
17. Kato T, Harada N, Ikeguchi-Ogura E, Sankoda A, Hatoko T, Lu X, Yasuda T, Yamane S, Inagaki N. Gene expression of nutrient-sensing molecules in L cells of CCK reporter male mice. *J Mol Endocrinol* 66: 11–22, 2021. doi:10.1530/JME-20-0134.
18. Suzuki K, Iwasaki K, Murata Y, Harada N, Yamane S, Hamasaki A, Shibue K, Joo E, Sankoda A, Fujiwara Y, Hayashi Y, Inagaki N. Distribution and hormonal characterization of primary murine L cells throughout the gastrointestinal tract. *J Diabetes Investig* 9: 25–32, 2018. doi:10.1111/jdi.12681.
19. Conwell DL, Zuccaro G, Morrow JB, Van Lente F, Obuchowski N, Vargo JJ, Dumot JA, Trolli P, Shay SS. Cholecystokinin-stimulated peak lipase concentration in duodenal drainage fluid: a new pancreatic function test. *Am J Gastroenterol* 97: 1392–1397, 2002. doi:10.1111/j.1572-0241.2002.05675.x.
20. Liddle RA, Goldfine ID, Rosen MS, Taplitz RA, Williams JA. Cholecystokinin bioactivity in human plasma. Molecular forms, responses to feeding, and relationship to gallbladder contraction. *J Clin Invest* 75: 1144–1152, 1985. doi:10.1172/JCI111809.
21. Yamane S, Harada N, Inagaki N. Mechanisms of fat-induced gastric inhibitory polypeptide/glucose-dependent insulinotropic polypeptide secretion from K cells. *J Diabetes Investig* 7: 20–26, 2016. doi:10.1111/jdi.12467.
22. Nasteska D, Harada N, Suzuki K, Yamane S, Hamasaki A, Joo E, Iwasaki K, Shibue K, Harada T, Inagaki N. Chronic reduction of GIP secretion alleviates obesity and insulin resistance under high-fat diet conditions. *Diabetes* 63: 2332–2343, 2014. doi:10.2337/db13-1563.
23. Lo CM, King A, Samuelson LC, Kindel TL, Rider T, Jandacek RJ, Raybould HE, Woods SC, Tso P. Cholecystokinin knockout mice are resistant to high-fat diet-induced obesity. *Gastroenterology* 138: 1997–2005, 2010. doi:10.1053/j.gastro.2010.01.044.
24. Kishikawa A, Kitaura H, Kimura K, Ogawa S, Qi J, Shen WR, Ohori F, Noguchi T, Marahleh A, Nara Y, Ichimura A, Mizoguchi I. Docosahexaenoic acid inhibits inflammation-induced osteoclast formation and bone resorption in vivo through GPR120 by inhibiting TNF- α production in macrophages and directly inhibiting osteoclast formation. *Front Endocrinol (Lausanne)* 10: 157, 2019. doi:10.3389/fendo.2019.00157.
25. Ikeguchi E, Harada N, Kanemaru Y, Sankoda A, Yamane S, Iwasaki K, Imajo M, Murata Y, Suzuki K, Joo E, Inagaki N. Transcriptional factor Pdx1 is involved in age-related GIP hypersecretion in mice. *Am J Physiol Gastrointest Liver Physiol* 315: G272–G282, 2018. doi:10.1152/ajpgi.00054.2018.
26. Ogawa E, Hosokawa M, Harada N, Yamane S, Hamasaki A, Toyoda K, Fujimoto S, Fujita Y, Fukuda K, Tsukiyama K, Yamada Y, Seino Y, Inagaki N. The effect of gastric inhibitory polypeptide on intestinal glucose absorption and intestinal motility in mice. *Biochem Biophys Res Commun* 404: 115–120, 2011. doi:10.1016/j.bbrc.2010.11.077.
27. Maekawa R, Seino Y, Ogata H, Murase M, Iida A, Hosokawa K, Joo E, Harada N, Tsunekawa S, Hamada Y, Oiso Y, Inagaki N, Hayashi Y, Arima H. Chronic high-sucrose diet increases fibroblast growth factor 21 production and energy expenditure in mice. *J Nutr Biochem* 49: 71–79, 2017. doi:10.1016/j.jnutbio.2017.07.010.
28. Furukawa I, Kurooka S, Arisue K, Kohda K, Hayashi C. Assays of serum lipase by the “BALB-DTNB method” mechanized for use with discrete and continuous-flow analyzers. *Clin Chem* 28: 110–113, 1982. doi:10.1093/clinchem/28.1.110.
29. Folch J, Lees M, Sloane Stanley GH. A simple method for the isolation and purification of total lipides from animal tissues. *J Biol Chem* 226: 497–509, 1957. doi:10.1016/S0021-9258(18)64849-5.
30. Kawasaki Y, Harashima S, Sasaki M, Mukai E, Nakamura Y, Harada N, Toyoda K, Hamasaki A, Yamane S, Yamada C, Yamada Y, Seino Y, Inagaki N. Exendin-4 protects pancreatic beta cells from the cytotoxic effect of rapamycin by inhibiting JNK and p38 phosphorylation. *Horm Metab Res* 42: 311–317, 2010. doi:10.1055/s-0030-1249035.
31. Galic S, Sachithanandan N, Kay TW, Steinberg GR. Suppressor of cytokine signalling (SOCS) proteins as guardians of inflammatory responses critical for regulating insulin sensitivity. *Biochem J* 461: 177–188, 2014. doi:10.1042/BJ20140143.
32. Trengove MC, Ward AC. SOCS proteins in development and disease. *Am J Clin Exp Immunol* 2: 1–29, 2013.
33. Ueki K, Kondo T, Tseng YH, Kahn CR. Central role of suppressors of cytokine signaling proteins in hepatic steatosis, insulin resistance, and the metabolic syndrome in the mouse. *Proc Natl Acad Sci U S A* 101: 10422–10427, 2004 [Erratum in *Proc Natl Acad Sci USA* 102: 13710, 2005]. doi:10.1073/pnas.0402511101.
34. Parker HE, Habib AM, Rogers GJ, Gribble FM, Reimann F. Nutrient-dependent secretion of glucose-dependent insulinotropic polypeptide from primary murine K cells. *Diabetologia* 52: 289–298, 2009. doi:10.1007/s00125-008-1202-x.
35. Sankoda A, Harada N, Kato T, Ikeguchi E, Iwasaki K, Yamane S, Murata Y, Hirasawa A, Inagaki N. Free fatty acid receptors, G protein-coupled receptor 120 and G protein-coupled receptor 40, are essential for oil-induced gastric inhibitory polypeptide secretion. *J Diabetes Investig* 10: 1430–1437, 2019. doi:10.1111/jdi.13059.
36. Wu T, Bound MJ, Standfield SD, Gedulin B, Jones KL, Horowitz M, Rayner CK. Effects of rectal administration of taurocholic acid on glucagon-like peptide-1 and peptide YY secretion in healthy

- humans. *Diabetes Obes Metab* 15: 474–477, 2013. doi:10.1111/dom.12043.
37. **Wu T, Bound MJ, Standfield SD, Jones KL, Horowitz M, Rayner CK.** Effects of taurocholic acid on glycemic, glucagon-like peptide-1, and insulin responses to small intestinal glucose infusion in healthy humans. *J Clin Endocrinol Metab* 98: E718–E722, 2013. doi:10.1210/jc.2012-3961.
 38. **Joo E, Harada N, Yamane S, Fukushima F, Taura D, Iwasaki K, Sankoda A, Shibue K, Harada T, Suzuki K, Hamasaki A, Inagaki N.** Inhibition of gastric inhibitory polypeptide receptor signaling in adipose tissue reduces insulin resistance and hepatic steatosis in high-fat diet-fed mice. *Diabetes* 66: 868–879, 2017. doi:10.2337/db16-0758.
 39. **Shimazu-Kuwahara S, Harada N, Yamane S, Joo E, Sankoda A, Kieffer TJ, Inagaki N.** Attenuated secretion of glucose-dependent insulinotropic polypeptide (GIP) does not alleviate hyperphagic obesity and insulin resistance in ob/ob mice. *Mol Metab* 6: 288–294, 2017. doi:10.1016/j.molmet.2017.01.006.
 40. **Yamane S, Harada N, Hamasaki A, Muraoka A, Joo E, Suzuki K, Nasteska D, Tanaka D, Ogura M, Harashima S, Inagaki N.** Effects of glucose and meal ingestion on incretin secretion in Japanese subjects with normal glucose tolerance. *J Diabetes Investig* 3: 80–85, 2012. doi:10.1111/j.2040-1124.2011.00143.x.
 41. **Suzuki K, Harada N, Yamane S, Nakamura Y, Sasaki K, Nasteska D, Joo E, Shibue K, Harada T, Hamasaki A, Toyoda K, Nagashima K, Inagaki N.** Transcriptional regulatory factor X6 (Rfx6) increases gastric inhibitory polypeptide (GIP) expression in enteroendocrine K-cells and is involved in GIP hypersecretion in high-fat diet-induced obesity. *J Biol Chem* 288: 1929–1938, 2013. doi:10.1074/jbc.M112.423137.
 42. **Miyawaki K, Yamada Y, Ban N, Ihara Y, Tsukiyama K, Zhou H, Fujimoto S, Oku A, Tsuda K, Toyokuni S, Hiai H, Mizunoya W, Fushiki T, Holst JJ, Makino M, Tashita A, Kobara Y, Tsubamoto Y, Jinnouchi T, Jomori T, Seino Y.** Inhibition of gastric inhibitory polypeptide signaling prevents obesity. *Nat Med* 8: 738–742, 2002. doi:10.1038/nm727.
 43. **Ibrahim MM.** Subcutaneous and visceral adipose tissue: structural and functional differences. *Obes Rev* 11: 11–18, 2010. doi:10.1111/j.1467-789X.2009.00623.x.
 44. **Moschen AR, Molnar C, Geiger S, Graziadei I, Ebenbichler CF, Weiss H, Kaser S, Kaser A, Tilg H.** Anti-inflammatory effects of excessive weight loss: potent suppression of adipose interleukin 6 and tumour necrosis factor alpha expression. *Gut* 59: 1259–1264, 2010. doi:10.1136/gut.2010.214577.
 45. **Sabio G, Das M, Mora A, Zhang Z, Jun JY, Ko HJ, Barrett T, Kim JK, Davis RJ.** A stress signaling pathway in adipose tissue regulates hepatic insulin resistance. *Science* 322: 1539–1543, 2008. doi:10.1126/science.1160794.
 46. **Johnston JA, O’Shea JJ.** Matching SOCS with function. *Nat Immunol* 4: 507–509, 2003. doi:10.1038/ni0603-507.
 47. **Murata Y, Harada N, Kishino S, Iwasaki K, Ikeguchi-Ogura E, Yamane S, Kato T, Kanemaru Y, Sankoda A, Hatoko T, Kiyobayashi S, Ogawa J, Hirasawa A, Inagaki N.** Medium-chain triglycerides inhibit long-chain triglyceride-induced GIP secretion through GPR120-dependent inhibition of CCK. *iScience* 24: 102963, 2021. doi:10.1016/j.isci.2021.102963.
 48. **Murata Y, Harada N, Yamane S, Iwasaki K, Ikeguchi E, Kanemaru Y, Harada T, Sankoda A, Shimazu-Kuwahara S, Joo E, Poudyal H, Inagaki N.** Medium-chain triglyceride diet stimulates less GIP secretion and suppresses body weight and fat mass gain compared with long-chain triglyceride diet. *Am J Physiol Endocrinol Physiol* 317: E53–E64, 2019 [Erratum in *Am J Physiol Endocrinol Physiol* 318: E440, 2020]. doi:10.1152/ajpendo.00200.2018.